

## Piezoelectric-field-induced localization of barrier states in {211}-oriented InAs/GaAs superlattices

P. Castrillo, M. I. Alonso,\* and G. Armelles

*Centro Nacional de Microelectrónica, Consejo Superior de Investigaciones Científicas, Serrano 144, E-28006 Madrid, Spain*

M. Ilg and K. Ploog<sup>†</sup>

*Max-Planck-Institut für Festkörperforschung, Heisenbergstrasse 1, W-7000 Stuttgart 80, Germany*

(Received 28 September 1992; revised manuscript received 20 January 1993)

We observe localized states whose energy is resonant with the continuum in GaAs with periodically inserted {211}-InAs sheets. Evidence for these states comprises excitonic interband transitions above the gap of GaAs, observed by piezoreflectance and photoluminescence-excitation spectroscopies. This localization has its origin in the strain-induced electric field existing in the InAs layers, which we show by simulations of the dielectric function based on envelope-function-type calculations.

Semiconductor superlattices (SL's) under external electric fields exhibit physical phenomena not observed in bulk semiconductors, such as Stark-ladder states and field-induced localization of eigenstates.<sup>1</sup> These phenomena result from the loss of coherence, caused by the electric field, between states of neighboring wells in the SL. Large built-in electric fields are produced in strained-layer SL's of III-V semiconductors grown along piezoelectric axes of the zinc-blende structure.<sup>2</sup> In these kinds of SL's, the potential profile is modified in a way different from that given by application of an external electric field, since the electric-field vector depends on the strain status of each particular layer, giving unique properties to piezoelectric SL's.<sup>2-5</sup> Recently, extremely thin InAs sheets embedded in GaAs have been shown to be piezoelectrically active.<sup>6</sup> In this paper, we present results of piezoreflectance (PZR) and photoluminescence excitation (PLE) spectroscopies which provide experimental evidence for localization of states induced by internal electric fields. In this case, the loss of coherence takes place between states of neighboring barriers, thus inducing localization of states with energies resonant with the continuum.

The experiments reported here were done on two InAs/GaAs SL's grown by molecular-beam epitaxy on {211} A GaAs substrates using optimized heating-cooling cycles for the deposition of the different layers. *In situ* monitoring by means of reflection high-energy electron diffraction showed a flat growth front of all times. The superlattices consist of ten periods of strained InAs thin layers separated by about 200 Å unstrained GaAs. The precise parameters of each sample were determined by double-crystal x-ray diffraction. The thicknesses of the InAs layers were 1.1 Å in one sample and 2.4 Å in the other. Details on the growth procedure and the structural and optical properties of the resulting samples have been published previously.<sup>6,7</sup> In order to perform PZR measurements the sample substrates were thinned to 150 μm and glued onto a piezoelectric transducer, which was driven by a modulated voltage. For the PLE measurements the sample was excited by a tunable cw dye laser. All spectra were taken at 80 K using standard experimental setups.

In Fig. 1 we compare two spectra of the sample with 2.4-Å-thick InAs layers. Curve (a) is a PZR spectrum and curve (b) is the numerical derivative of the reflectance with respect to the energy. The latter spectrum is equivalent to a wavelength-modulated reflectance spectrum. Both spectra clearly display the same features with the same relative intensities between them. This implies that all observed transitions have the same character, in contrast to spectra taken from {100}-oriented samples where two transitions of different character, i.e., light and heavy hole, are observed.<sup>8</sup> In addition, we know from this comparison that, for these samples, stress modulation is equivalent to energy modulation and that any other modulation mechanism is very weak. This conclusion is valid for both samples studied here, those spectra look very similar. We distinguish two regions in the PZR spectra. The energy region below the substrate signature (labeled 2 in Fig. 1) shows a feature (labeled 1) containing one or more transitions originating from

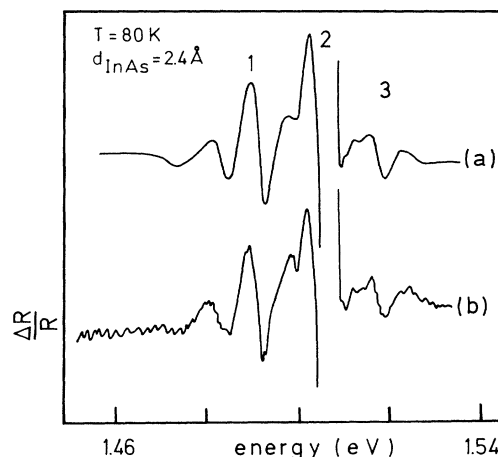


FIG. 1. Experimental spectra for the sample with  $d_{\text{InAs}} = 2.4 \text{ \AA}$ : (a) piezoreflectance, (b) numerical derivative of reflectance spectrum with respect to the energy. Labels 1–3 correspond to the observed features (see text). The strong transition labeled 2 is assigned to bulk GaAs and is left out of scale.

bound states associated either to the InAs or to the GaAs layers. The energy region above the free-exciton transition of bulk GaAs exhibits an additional feature (labeled 3) around 1.520 eV. We concentrate now on this higher-energy region. The mentioned structure is observed even in the sample with thinner InAs layers, whose PZR spectrum is shown in Fig. 2. In contrast, it does not appear in modulated spectra of  $\{100\}$ -InAs/GaAs SL's.<sup>9</sup> Figure 3 shows a PLE spectrum taken from the sample of Fig. 1 with the detection energy set at 1.483 eV. The corresponding photoluminescence peak coincides approximately in energy with the spectral feature labeled 1 in Fig. 1. In the PLE spectrum, an excitonic peak superimposed on the continuum is observed at 1.521 eV, which is about the energy position of the feature labeled 3 in Fig. 1. This peak shows up always at the same energy, independently of the detection energy. It is only seen for low excitation intensities and it merges into the continuum when the power of the exciting laser is increased.

In order to understand the origin of the excitonic transitions observed in the spectra, we made a calculation within the envelope-function approximation, by applying the transfer-matrix formalism to the ten-period potential profile of our samples. We determine both the heavy-hole and electron envelope functions to calculate their overlap. The shape of the potential taken in the calculation is shown in Fig. 4. It has staircase form except for the InAs wells. The magnitude of the built-in electric field in the InAs sheets determines the riser ( $V_s$ ) of the steps, whereas the width of the treads ( $L_t$ ) is given by the thickness of the GaAs barriers. The results presented here are obtained with the parameters of the sample with  $d_{\text{InAs}} = 2.4 \text{ \AA}$ . Using this thickness, the strain present in the InAs layer, and the piezoelectric constants of InAs,<sup>10</sup> we obtain a riser of  $V_s = 7 \text{ meV}$ . However, we have to take into account the presence of In segregation experimentally found in these samples,<sup>7</sup> which can enlarge  $V_s$  due to the large difference between the piezoelectric constants of InAs and GaAs.<sup>11</sup> Therefore we performed calculations for  $V_s$  in the range from 7 to 25 meV. The tread width is  $L_t = 230 \text{ \AA}$  for this particular sample. The InAs wells were considered as  $\delta$ -function potentials. In

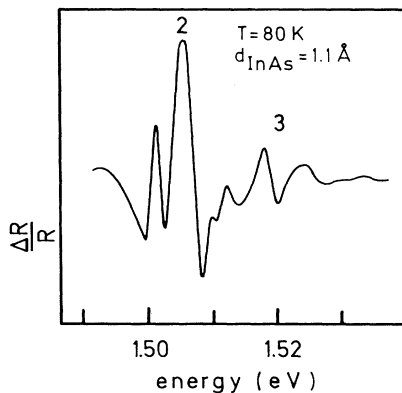


FIG. 2. Piezoreflectance spectrum measured in the sample with 1.1- $\text{\AA}$ -thick InAs layers. The observed features are labeled as in Fig. 1.

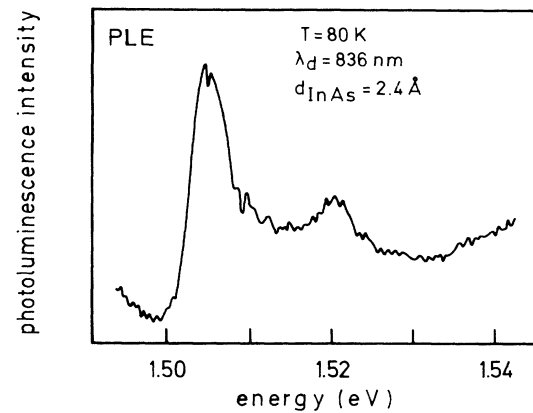


FIG. 3. Photoluminescence excitation spectrum of the sample in Fig. 1 detected at  $\lambda_d = 836 \text{ nm}$  ( $E_d = 1.483 \text{ eV}$ ).

this way, we avoid explicit description of the potential profiles of the InAs sheets, which are not well known due to the above-mentioned segregation and to the uncertainty about the band offsets in our  $\{211\}$  strained system. This  $\delta$ -function approximation is justified for the case of ultrathin wells, in which the envelope wave functions of

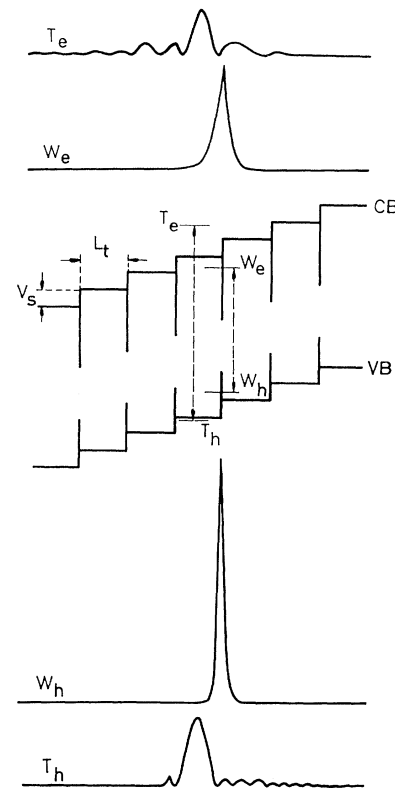


FIG. 4. Schematic diagram of the potential profile for conduction and valence bands (CB and VB) used in the calculation. The relevant energy levels and their respective squared envelope functions, calculated for  $\delta$ -function potentials with the parameters described in the text, are also shown. These functions are all displayed on the same scale  $T_e$  and  $W_e$  are for electrons,  $W_h$  and  $T_h$  for holes.

states spread mainly on the barriers. This is especially valid for unbound states. Effective masses and energy gap used for GaAs are  $m_e=0.066$ ,  $m_{hh}=0.50$ , and  $E_g=1.505$  eV. From the calculation we obtain two types of localized functions giving rise to excitonic transitions. Figure 4 displays the envelope probability densities, both for electrons and holes, calculated for  $V_s=11$  meV.  $\delta$ -function magnitudes were chosen such that the binding energies of bound states associated with the wells amount to 6.5 meV for electrons (level  $W_e$ ) and 5.0 meV for holes (level  $W_h$ ). These binding energies are the same as the ones obtained for a system containing homogeneously segregated 3-Å-thick  $\text{Ga}_{0.2}\text{In}_{0.8}\text{As}$  wells, for which the obtained riser is also 11 meV.<sup>12</sup>

In addition, we find states with energies in the continuum that have envelope functions localized at the treads of the potential. The energies of these tread states, also shown in Fig. 4, are 18.5 meV above the tread for electrons (level  $T_e$ ) and 1.8 meV for holes (level  $T_h$ ). While both the energies and the envelope functions of the bound states  $W_e$  and  $W_h$  are almost independent of the riser (magnitude of the electric field), the tread states  $T_e$  and  $T_h$  are clearly induced by the presence of this field. A decrease of the riser provokes the tread energy levels to interact, thus forming a miniband, while the envelope functions concomitantly delocalize and merge into the continuum. In our calculation, we did not take into account the excitonic interaction between electron and hole states. Such interaction should both increase the intensity and reduce the energy of localized transitions.

PZR spectra are related with the derivative of the dielectric function affected by a phase factor. In our experimental conditions, Gaussian line shapes seem to be the most likely for excitonic transitions.<sup>13</sup> Figure 5 shows the derivatives of real and imaginary parts of the dielectric function calculated by using Gaussian line shapes from the overlap of the four kinds of localized envelope functions shown in Fig. 4. The strongest features arise from bound-to-bound ( $W_e$ - $W_h$ ) and tread-to-tread ( $T_e$ - $T_h$ ) transitions. As a consequence, we assign the feature labeled 3 in Fig. 1 to the transition  $T_e$ - $T_h$  between tread states and feature 1 to transition  $W_e$ - $W_h$  between bound states. Some features arising from bound-to-tread transitions ( $W_e$ - $T_h$  and  $T_e$ - $W_h$ ) are observed in the calculated

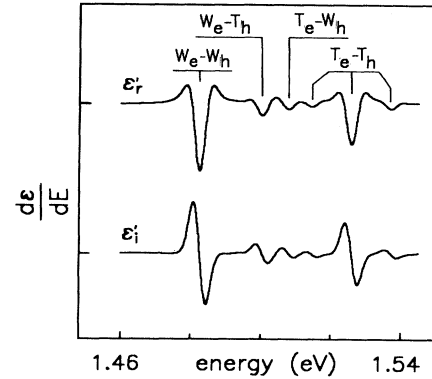


FIG. 5. Real ( $\epsilon'_r$ ) and imaginary ( $\epsilon'_i$ ) parts of the derivative dielectric function ( $d\epsilon/dE$ ) calculated from the overlap of localized electron and hole envelope functions shown in Fig. 4.  $W_e$ - $W_h$ ,  $W_e$ - $T_h$ ,  $T_e$ - $W_h$ , and  $T_e$ - $T_h$  label the significant transitions between the states displayed in Fig. 4. Features related to  $T_e$ - $T_h$  Stark-ladder transitions can also be observed.

spectra, but they are not conclusively resolved in Fig. 1 due to the large intensity of the substrate feature. Features related to transitions between adjacent barriers ( $T_e$ - $T_h$  Stark-ladder transitions) can also be observed in the calculated spectra. The calculation predicts negligible intensities for the other Stark-ladder transitions, due to the large thickness of the GaAs barriers.

The dielectric function calculated on the basis of our simple approximation qualitatively accounts very well for the features related to states resonating with the continuum observed in the PZR spectra.

In summary, we have presented experimental evidence of localized barrier states induced by the built-in electric field in strained-layer piezoelectric  $\{211\}$ -InAs/GaAs SL's. In addition, our results reinforce previous data<sup>6</sup> that suggested the existence of such fields in the ultimate atomic limit, and show the potential of this type of structure for studying new physical phenomena.

This work has been supported in part by CICYT under Project No. MAT92-0262.

\*Present address: Institut de Ciència de Materials de Barcelona, CSIC, E-08193 Bellaterra, Spain.

†Present address: Paul-Drude-Institut für Festkörperelektronik, O-1086 Berlin, Germany.

<sup>1</sup>E. E. Méndez, F. Agulló-Rueda, and J. M. Hong, Phys. Rev. Lett. **60**, 2426 (1988).

<sup>2</sup>D. L. Smith and C. Mailhot, Phys. Rev. Lett. **58**, 1264 (1987).

<sup>3</sup>B. K. Laurich, K. Elcess, G. G. Fonstad, J. G. Beery, C. Mailhot, and D. L. Smith, Phys. Rev. Lett. **62**, 649 (1989).

<sup>4</sup>E. A. Caridi, T. Y. Chang, K. W. Goosen, and L. F. Eastman, Appl. Phys. Lett. **56**, 659 (1990).

<sup>5</sup>I. Sela, D. E. Watkins, B. K. Laurich, D. L. Smith, S. Subanna, and H. Kroemer, Appl. Phys. Lett. **58**, 684 (1991).

<sup>6</sup>M. Ilg, O. Brandt, A. Ruiz, and K. Ploog, Phys. Rev. B **45**, 8825 (1992).

<sup>7</sup>M. Ilg, O. Brandt, and K. Ploog, Appl. Phys. Lett. **61**, 441 (1992).

<sup>8</sup>P. Castrillo, G. Armelles, A. Ruiz, and F. Briones, Jpn. J. Appl. Phys. **30**, L1784 (1991).

<sup>9</sup>R. Cingolani, O. Brand, L. Tapfer, G. Scamarcio, G. C. La Rocca, and K. Ploog, Phys. Rev. B **42**, 3209 (1990).

<sup>10</sup>Numerical Data and Functional Relationships in Science and Technology, edited by O. Madelung, Landolt-Börnstein New Series, Vol. 17 (Springer, Berlin, 1982).

<sup>11</sup>The piezoelectric constants for InAs and GaAs are  $e_{14}$  (InAs) =  $-0.045$  C/m<sup>2</sup> and  $e_{14}$  (GaAs) =  $-0.16$  C/m<sup>2</sup>. For the  $\text{Ga}_{1-x}\text{In}_x\text{As}$  alloy, we assume a linear interpolation between the bulk material parameters. Then, the riser produced by a 12-Å-thick  $\{211\}$ - $\text{Ga}_{0.8}\text{In}_{0.2}\text{As}$  layer (matched to GaAs) is 25 meV, more than three times larger than that produced by a

2.4-Å-thick {211}-InAs layer, in spite of both structures having the same average In content.

<sup>12</sup>For these calculations we used  $E_g = 0.53$  eV,  $m_e = 0.024$ , and  $m_{hh} = 0.41$ , for InAs, and an interpolation between InAs and GaAs parameters for the  $\text{Ga}_{1-x}\text{In}_x\text{As}$  alloy generated by

segregation. We have used a conduction-band offset of 75%.

<sup>13</sup>See, for example, W. M. Theis, G. D. Sanders, C. E. Leak, K. K. Bajaj, and H. Morkoç, *Phys. Rev. B* **37**, 3042 (1988), and references therein.